Electrical transport properties of Cr-Si and Cr-Ga alloy single crystals

1998 J. Phys.: Condens. Matter 10 2715

(http://iopscience.iop.org/0953-8984/10/12/011)

J. Phys.: Condens. Matter **10** (1998) 2715–2725. Printed in the UK PII: S0953-8984(98)89587-8

Electrical transport properties of Cr–Si and Cr–Ga alloy single crystals

A R E Prinsloo, H L Alberts and P Smit

Department of Physics, Rand Afrikaans University, PO Box 524, Auckland Park, Johannesburg 2006, South Africa

Received 27 November 1997

Abstract. Measurements are reported of the electrical resistivity of dilute Cr–Si and Cr–Ga alloy single crystals in the temperature range 4 to 1000 K. Analyses of the data show large magnetic contributions to the electrical resistivity of all of the alloys at temperatures $0 < T < 2T_N$, where T_N is the Néel temperature. These magnetic contributions are partly attributed to spin-fluctuation and temperature-dependent resonant impurity scattering effects. A hysteretic resistivity anomaly, ascribed to the effects of mixed incommensurate (I) and commensurate (C) spin-density-wave (SDW) states, was observed near the I–C phase transition temperature of Cr + 1.2 at.% Si. The resistivity of Cr + 0.16 at.% Ga shows a small and unusual anomaly near the spin-flip transition temperature.

1. Introduction

There is renewed interest in the electrical transport properties of dilute Cr alloys, particularly in those of alloys containing nonmagnetic impurities [1–8]. Recently Galkin and co-workers [1–8] performed very interesting experiments on the electrical resistivity of ternary polycrystalline Cr–Si–Mn and Cr–Si–V alloys. They demonstrated the importance of resonant scattering of conduction electrons at local impurity states within the spin-density-wave (SDW) energy gap, in the electrical resistivity (ρ) of Cr–Si alloys. The resonant impurity scattering mechanism is believed [2] to be also of importance in dilute Cr alloys with other sp nonmagnetic impurities, like for instance in Cr–Ga alloys whose magnetic phase diagram somewhat resembles that of the Cr–Si system [2, 7]. Here sp refers to the 3s and 3p electron shells of the impurity atom.

In a study of the electrical resistivity of dilute Cr alloys it is of importance to separate the nonmagnetic component of ρ from the other contributions. These other contributions include contributions from the reduction of the number of current carriers by the appearance of the SDW energy gap in the electron energy spectrum at temperatures below the Néel temperature (T_N), from the resonant impurity scattering of electrons and from spin-fluctuation effects. Studies by Chiu *et al* [9] on Cr–Ti alloys show that magnetic excitations exist in Cr alloys up to temperatures as high as $1.5T_N$ or higher (see also reference [10]). This means that measurements on dilute Cr alloys, like Cr–Si and Cr–Ga, should be done up to about 1000 K to allow for a proper back-extrapolation from the paramagnetic region down to 0 K in order to determine the nonmagnetic component of ρ. Previous measurements on Cr–Si [11] and Cr–Ga [12, 13] alloys concentrated mainly on the behaviour of ρ at the magnetic phase transition temperatures T_N and the incommensurate-to-commensurate (I–C) SDW transition temperature T_{IC}. The measurements were done on polycrystalline alloys and were done

0953-8984/98/122715+11$19.50

only up to about 320 K in the case of Cr–Si [11] and up to about 450 K for Cr–Ga [13] alloys. These temperatures are unfortunately not high enough for obtaining the nonmagnetic component for each of these alloy systems correctly.

We [14–16] recently succeeded in growing good quality Cr–Si and Cr–Ga alloy single crystals and ρ–T measurements up to about 1000 K on these crystals are reported here. Three Cr–Si and three Cr–Ga alloy single crystals were studied. For the Cr–Si system the concentration of one of the crystals is below the triple-point concentration (c_t), where the CSDW, ISDW and paramagnetic (P) states coexist, and for the other two $c > c_t$. For the Cr–Ga system two crystals with $c < c_t$ and one with $c > c_t$ were studied. Cr alloys with $c > c_t$ show both ISDW–CSDW, at T_{IC}, and CSDW–P, at T_N, transitions, while alloys with $c < c_t$ show no ISDW–CSDW transition and an ISDW–P Néel transition.

2. Experimental methods

The Cr–Ga [14] and Cr–Si [15, 16] single crystals used in the present study are the same crystals as were previously used for measurements of the temperature dependence of the elastic constants and thermal expansion. The single crystals were grown by a floating-zone technique using radio-frequency heating as previously described [16]. The starting materials were polycrystalline rods prepared from 99.996% pure Cr, 99.999% pure Ga and 99.999% pure Si. The actual concentrations of 0.16 ± 0.06 at.% Ga, 0.42 ± 0.03 at.% Ga and 0.88 ± 0.06 at.% Ga for the three Cr–Ga crystals were determined using electron microprobe analysis techniques. Using the same technique the nominal concentrations of 0.5 at.% Si, 1.2 at.% Si and 1.6 at.% Si were found to differ by less than 6% from the actual concentrations of the Cr–Si alloy single crystals. Electrical resistivity was measured using a standard four-probe DC method for both forward and reverse current directions in order to eliminate thermal emfs. The sample lengths were about 7 mm and the cross sectional area about 1 mm^2. The longest axis was directed along [100] for all of the crystals. The Cr–Ga and Cr–Si crystals in this study were in the multi-$\boldsymbol{Q}$ domain state, meaning that they consist of magnetic domains below T_N in which the SDW $\boldsymbol{Q}$-vector in each is directed at random along any one of the six equivalent [100] directions. Furthermore, since the crystals are of cubic structure and electrical conductivity is represented by a tensor of the second rank, we do not expect [17] anisotropy of the electrical resistivity in these alloys. Current was applied along the long axis of the sample and data were recorded during both heating and cooling runs in the temperature range 77 to 1000 K as well as at a constant temperature of 4.2 K. During heating runs from 77 to 1000 K, data were recorded at $\approx$0.05 K intervals while heating the sample slowly at less than 0.5 K min^{-1}. The cooling rate was the same and data were recorded at the same intervals.

3. Results

Figures 1(a), 1(b) and 1(d) show ρ as a function of temperature on heating between 77 and 1000 K, as well as values obtained at 4.2 K, for the Cr + 0.5 at.% Si, Cr + 1.2 at.% Si and Cr + 1.6 at.% Si samples, respectively. Figures 1(c) and 1(e) show, respectively, the detailed behaviour observed during cooling and heating runs in the temperature region 77–350 K for the Cr + 1.2 at.% Si and Cr + 1.6 at.% Si alloy crystals. Both of these alloys show step-like first-order transitions, accompanied by hysteresis effects, in the ρ–T curves at T_N. The hysteresis width at T_N for these two crystals is between 3 and 5 K which is roughly the same as that obtained for the same crystals using ultrasonic and thermal

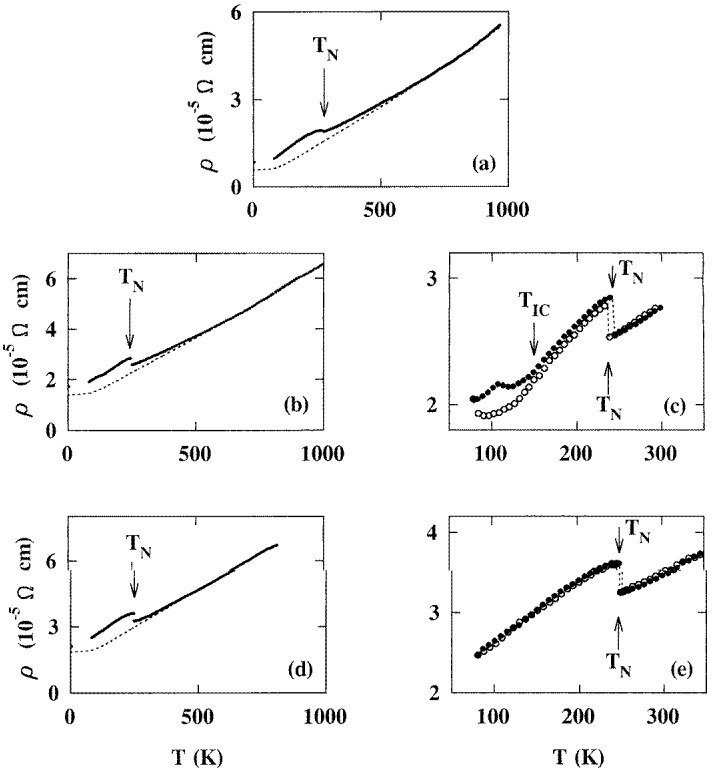

Figure 1. The electrical resistivity, ρ, as a function of the temperature for Cr–Si alloy single crystals with (a) 0.5 at.% Si, (b) 1.2 at.% Si and (d) 1.6 at.% Si. The data points in (a), (b) and (d) were recorded during heating runs. In each of these panels there is also a data point at 4.2 K. The broken lines in (a), (b) and (d) represent the ideal nonmagnetic resistivity of each Cr–Si alloy. (c) shows the detailed behaviour around T_{IC} and T_N for Cr + 1.2 at.% Si and (e) that around T_N for Cr + 1.6 at.% Si. In these two panels results obtained during a heating run are represented by ● and those obtained during a cooling run by ○. The value of T_{IC} shown in (c) was obtained from thermal expansion measurements [16]. In all of the measurements the current was directed along [100].

expansion measuring techniques [16]. Large hysteresis effects were observed in ρ–T for the Cr + 1.2 at.% Si crystal at low temperatures (figure 1(c)). This low-temperature hysteresis corresponds to that observed [16] in thermal expansion measurements on the same crystal, and is attributed [16] to the possibility of mixed ISDW/CSDW phases that may occur near the ISDW–CSDW phase transition of the Cr + 1.2 at.% Si crystal. One may expect that the mixed phases should also contribute to ρ near T_{IC}. Electrons may be scattered by the boundaries between the coexisting ISDW and CSDW domains, giving extra resistivity, similar to that [18, 19] predicted for electron scattering by Bloch walls in a ferromagnet. In a ferromagnet the domain walls are of a thickness that is generally [20] much greater than the electronic mean free path length. They therefore contribute only a relatively small component to the total resistivity, except at low temperatures. One does not know the size of this effect in the Cr–Si alloys. Apart from the effect described above, ρ may also change in going from the ISDW to the CSDW phase (on heating) due to an increase in nesting of the electron and hole Fermi surface sheets. The increase in nesting should give an increase

of ρ when the CSDW phase is entered above T_{IC}. The opposite happens in figure 1(c). The slightly larger ρ in the ISDW phase just below T_{IC} in figure 1(c) on heating can probably be ascribed to the effects of the boundaries between the mixed phases dominating the effects of the changes in nesting. The ISDW–CSDW transition temperature of the Cr + 1.6 at.% Si crystal is below 77 K and was not investigated in the present study.

T_N was taken for Cr + 1.2 at.% Si and Cr + 1.6 at.% Si at the middle of the sharp step-like transitions in figures 1(c) and 1(e). For Cr + 0.5 at.% Si for which $c < c_t$, the temperature of the minimum point, $T = 278 \pm 1$ K, on the ρ–T curve of figure 1(a) corresponds nearly exactly with T_N obtained from ultrasonic and thermal expansion measurements [16]. For this alloy T_N was thus taken at the temperature of this minimum. The values of T_N obtained from figures 1(a), 1(c) and 1(e) are: for Cr + 1.6 at.% Si, $T_N = 250.3 \pm 0.5$ K (on heating) and $T_N = 246.9 \pm 0.5$ K (on cooling); for Cr + 1.2 at.% Si, $T_N = 241.6 \pm 0.5$ K (on heating) and $T_N = 237.0 \pm 0.5$ K (on cooling); for Cr + 0.5 at.% Si, $T_N = 278 \pm 1$ K (no hysteresis). For Cr + 0.5 at.% Si and Cr + 1.6 at.% Si the values of T_N obtained in the present study, using ρ-measurements, compare very well with those obtained for the same crystals by Anderson *et al* [16] using ultrasonic and thermal expansion measurements. For the Cr + 1.2 at.% Si crystal, T_N in the present study is however about 10 K lower than the results obtained by Anderson *et al* [16]. The difference may partly be due to the different physical properties that were used to determine T_N in the two different studies.

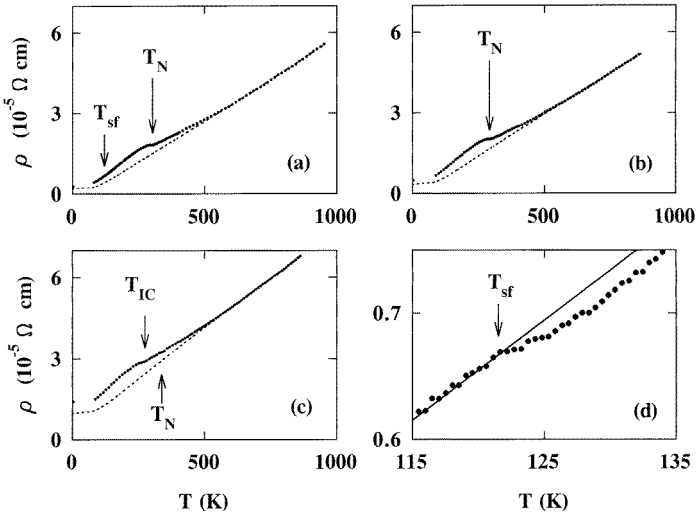

Figure 2. The electrical resistivity, ρ, as a function of the temperature for Cr–Ga alloy single crystals with (a) 0.16 at.% Ga, (b) 0.42 at.% Ga and (c) 0.88 at.% Ga. The data points in (a), (b) and (c) were recorded during heating runs. In each of these panels there is also a data point at 4.2 K. Heating and cooling runs show no hysteresis effects. The broken lines in (a), (b) and (c), obtained using $\alpha = 0.3$, represent the ideal nonmagnetic resistivity of each Cr–Ga alloy. (d) shows the detailed behaviour of ρ near the spin-flip transition temperature, T_{sf}, of Cr + 0.16 at.% Ga. The solid line in (d) is a guide to the eye added to make the ρ-anomaly at T_{sf} more visible.

Figures 2(a), 2(b) and 2(c) show ρ as a function of temperature in the temperature range 77–1000 K, as well as values at 4.2 K, for the Cr + 0.16 at.% Ga, Cr + 0.42 at.% Ga and Cr + 0.88 at.% Ga crystals, respectively. T_N for the Cr + 0.42 at.% Ga and Cr + 0.16 at.% Ga crystals was taken at the inflection point, below the minimum point,

on the ρ–T curve of each. This gives $T_N = 294 \pm 1$ K for Cr + 0.42 at.% Ga and $T_N = 300 \pm 1$ K for Cr + 0.16 at.% Ga. No hysteresis effects were observed near T_N for these two samples. The values of T_N compare well with values obtained [14] from thermal expansion and ultrasonic wave velocity measurements on the same crystals. Figure 2(d) shows a small anomaly just below 125 K, which corresponds to the spin-flip transition temperature $T_{sf} = 122 \pm 2$ K obtained from ultrasonic measurements [14]. Usually the spin-flip transitions from longitudinal (L) ISDW to transverse (T) ISDW do not give a ρ-anomaly for dilute Cr alloys [7]. The anomaly observed in figure 2(d) is in a sense an exception and suggests that ρ is a little smaller in the TISDW phase at $T > T_{sf}$ of Cr + 0.16 at.% Ga than in the extrapolated LISDW phase, extrapolated from $T < T_{sf}$ to $T > T_{sf}$ (the solid line in figure 2(d)), at the same temperature $T > T_{sf}$. It is hard to understand why the resistivity at $T > T_{sf}$ in the TISDW phase is a little smaller than the resistivity of the extrapolated LISDW phase (figure 2(d)). From simple reasoning one expects the opposite to be the case as an extra degree of freedom is available to the spin system at $T > T_{sf}$ when the spin polarization is transverse. The extra degree of freedom makes the spin system more disordered at $T > T_{sf}$, resulting in an increase in ρ on heating through T_{sf}. The opposite is observed in figure 2(d). Apparently there are other effects, currently unknown, that play a role in the observed behaviour near T_{sf}. For the Cr + 0.88 at.% Ga crystal, T_{IC} and T_N are very close together giving only a broad minimum in the $\mathrm{d}\rho/\mathrm{d}T$–$T$ curve. This complicates a determination of T_{IC} and T_N from the ρ–T curve in figure 2(c). These temperatures are better resolved in thermal expansion measurements [14] on this crystal. T_{IC} and T_N shown in figure 2(c) were obtained from such measurements [14]. Figure 3 shows the resistivity at 4.2 K measured for the Cr–Si alloy crystals together with values obtained by Arajs and Katzenmeyer [11] and the value for Cr + 1.3 at.% Si obtained by Galkin [1]. The ρ(4.2 K) values obtained in the three different studies compare very well, indicating samples of about the same quality for the different studies.

4. Discussion

4.1. Cr–Si alloys

Recent resistivity studies [1–8] on Cr–Si–V and Cr–Si–Mn alloys emphasize the role of resonant scattering of electrons by impurity levels formed within the SDW energy gap of dilute Cr–Si alloys. Galkin [1, 6, 8] doped a Cr + 1.3 at.% Si alloy with V to lower the Fermi energy (E_F) and with Mn to increase it, thereby 'tuning' E_F through the impurity levels. When E_F approaches the impurity level, the scattering of conduction electrons becomes resonant, resulting in peaks in the residual resistivity (in practice the resistivity at 4.2 K) at certain V or Mn doping concentrations. For Cr + 1.3 at.% Si, Galkin [1, 6, 8] showed experimentally that ρ(4.2 K) shows a broad peak at around 0.2 at.% V doping and a fairly sharp peak at around 0.6 at.% Mn doping. At low temperatures, $kT \ll \gamma$, where γ is the half-width of the impurity levels, resonant impurity scattering contributes a term ρ_{res}^0, which is temperature independent, and a negative temperature-dependent term $\rho_{\mathrm{res}}(T)$ to the electrical resistivity [3, 7]. The term $\rho_{\mathrm{res}}(T)$ is responsible for the low-temperature minimum observed [1, 11] in the ρ–T curves of Cr–Si alloys.

Apart from the resonant impurity scattering contribution to the resistivity of Cr–Si alloys there are also contributions from nonresonant impurity scattering, electron–phonon scattering, the reduction of the number of current carriers due to the appearance of the SDW energy gap below T_N, and from effects of spin fluctuations. Combining all of the above

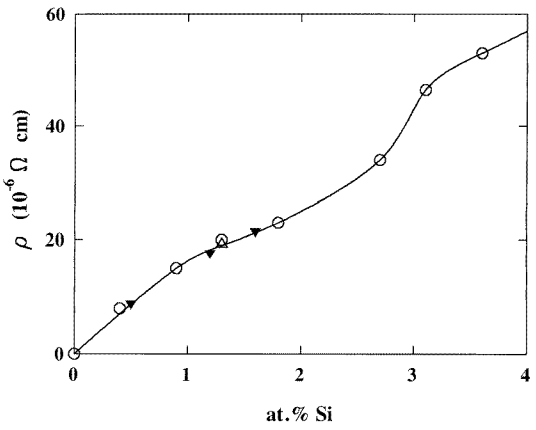

Figure 3. The residual resistivity, ρ, at 4.2 K as a function of the Si concentration for Cr–Si alloys. The points marked ○ were obtained from reference [11], the points marked ▼ are from the present study and the point △ was obtained from reference [1]. The solid line is a guide to the eye.

and using the approach of Chiu *et al* [9], we write the resistivity of Cr–Si alloys as

$$\rho_{\exp}(T) = \rho_{\text{res}}^0 + \rho_{\text{res}}(T) + \frac{\rho_0^0}{1-\alpha\,\Delta(T)/\Delta(0)} + \frac{\rho_{e-p}^P(T)}{1-\alpha\,\Delta(T)/\Delta(0)} + \frac{\rho_m(T)}{1-\alpha\,\Delta(T)/\Delta(0)}. \tag{1}$$

Here ρ_0^0 represents the residual resistivity at 0 K due to the normal potential scattering, while ρ_{e-p}^P represents the electron–phonon resistivity of an ideal nonmagnetic Cr alloy which is of the form

$$\rho_{e-p}^P = \frac{k}{\theta_D^2} T G(\theta_D/T) + BT^3. \tag{2}$$

Equation (2) includes [9] an electron s–d scattering term that is of importance for Cr alloys. G is the Grüneisen function [21], $\theta_D(T)$ is the temperature-dependent Debye temperature which was obtained for Cr–Si and Cr–Ga as explained previously [10] and k and B are constants. The factor $[1-\alpha\,\Delta(T)/\Delta(0)]$ in equation (1) appears because of the reduction in the number of current carriers due to the formation of the SDW below T_N. $\Delta(T)/\Delta(0)$ is [9] the BCS energy gap function as tabulated by Mühlschlegel [22]. $\rho_m(T)$ in equation (1) represents the resistivity due to spin-fluctuation effects and $\rho_{\text{res}}(T)$ is taken to give the temperature-dependent resonance scattering resistivity at any $T > 0$ K. At temperatures well above the Néel point in the paramagnetic phase where the SDW energy gap is absent, we expect the major contribution to $\rho_{\exp}(T)$ to be given by the term $\rho_{e-p}^P(T)$ of equation (2). Equation (2) can then be used to extrapolate the ρ–T curve of each Cr–Si crystal from high temperatures down to 0 K in order to obtain the ρ–T behaviour of the particular alloy if it was to remain in the ideal paramagnetic state at all $T > 0$ K. In order to do so one also needs to know the value, ρ_0^0, of the residual resistivity due to normal potential scattering for each alloy. ρ_0^0 represents the resistivity at 0 K of the ideal paramagnetic state of each Cr–Si alloy. We obtained ρ_0^0 for the Cr–Si alloys from the work of Galkin [1, 6, 8]. He measured the residual resistivity of a Cr + 1.3 at.% Si alloy doped with different concentrations of V. V suppresses the SDW antiferromagnetism in Cr + 1.3 at.% Si, making it paramagnetic

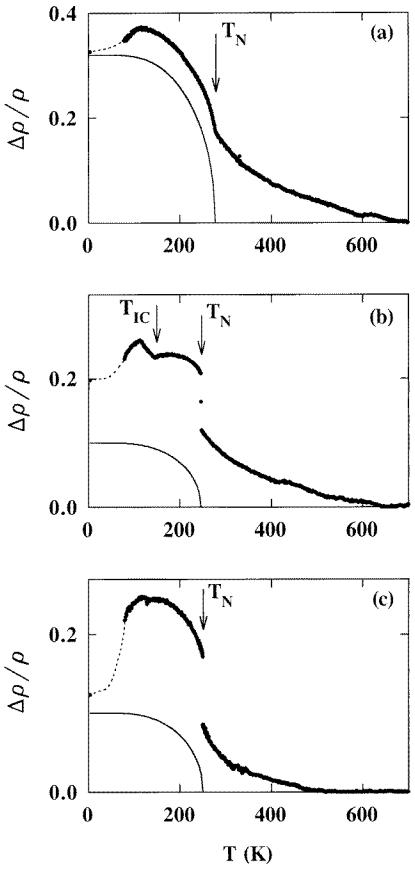

Figure 4. The resistivity anomaly, $\Delta\rho/\rho = [\rho_{\rm exp}(T) - \rho_{\rm nonmagn}(T)]/\rho_{\rm exp}(T)$, as a function of the temperature for (a) Cr + 0.5 at.% Si, (b) Cr + 1.2 at.% Si and (c) Cr + 1.6 at.% Si. The broken line connecting the measurements at 4.2 K with that at 77 K is a guide to the eye. The solid line in each panel represents the expected $\Delta\rho/\rho$ calculated by taking only nesting effects of the Fermi surface sheets into account. In (a) this calculation was done using $\alpha = 0.32$ and in (b) and (c) the value $\alpha = 0.1$ was used.

at all temperatures for V doping of more than about 1 at.% V [1, 2]. For paramagnetic $(Cr_{1-y}V_y)$–1.3 at.% Si alloys with y between 1 at.% and 5 at.%, Galkin [6] observed a roughly linear increase in the residual resistivity ($\rho_{\rm exp}$(4.2 K)) with increasing V content. By extrapolating this line back to $y = 0$ (figure 2 of reference [6]) one obtains ρ_0^0 for Cr + 1.3 at.% Si. The value obtained is ρ_0^0(Cr + 1.3 at.% Si) = 15.2 $\mu\Omega$ cm. For pure Cr, in the SDW state, for which the resonant impurity scattering effects are absent, it follows from equation (1) that $\rho_{\rm exp}(4.2\ {\rm K}) = \rho_0^0/(1-\alpha)$, where in practice $\rho_{\rm exp}(0) \approx \rho_{\rm exp}(4.2\ {\rm K})$. α is a measure of the fraction of the Fermi surface sheets at 0 K that are annihilated by the formation of the SDW [9]. For pure Cr we can take $\alpha \approx 0.3$ [9]. We measure $\rho_{\rm exp}(4.2\ {\rm K}) = 0.04\ \mu\Omega$ cm for pure Cr. This gives $\rho_0^0 = 0.03\ \mu\Omega$ cm. Since one expects ρ_0^0 for nonmagnetic dilute alloys to vary linearly with concentration [20], we obtained ρ_0^0 for our Cr–Si alloys from a linear extrapolation between $\rho_0^0 = 0.03\ \mu\Omega$ cm for pure Cr and $\rho_0^0 = 15.2\ \mu\Omega$ cm for Cr + 1.3 at.% Si. This gives ρ_0^0(Cr + 0.5 at.% Si) = 5.9 $\mu\Omega$ cm, ρ_0^0(Cr + 1.2 at.% Si) = 14.0 $\mu\Omega$ cm and ρ_0^0(Cr + 1.6 at.% Si) = 18.7 $\mu\Omega$ cm. Curves

of $[\rho_{\exp}(T) - \rho_0^0]/T^3$ versus $T^{-2}\theta_D^{-2}(T)G(\theta_D/T)$, where ρ_{e-p}^P in equation (2) at high temperatures is given by $\rho_{\exp}(T) - \rho_0^0$, were found to be straight lines for the present Cr–Si alloys in the temperature range 500 K to 1000 K. These straight lines allow us to obtain the constants k and B in equation (2) for the back-extrapolation to obtain the resistivity $\rho^P(T)$ of the ideal nonmagnetic alloy from $\rho^P(T) = \rho_0^0 + \rho_{e-p}^P$. The back-extrapolations are shown by the broken lines in figures 1(a), 1(b) and 1(d). The resistivity anomaly $\Delta\rho(T)/\rho(T) = [\rho_{\exp}(T) - \rho^P(T)]/\rho_{\exp}(T)$, obtained from figures 1(a), 1(b) and 1(d) for the three Cr–Si crystals, is shown in figure 4.

At 0 K (in practice 4.2 K), $\rho_{\exp}(0)$ for a Cr–Si alloy is given by

$$\rho_{\exp}(0) = \rho_{\text{res}}^0 + \frac{\rho_0^0}{1-\alpha}. \tag{3}$$

We used the following arguments to make a rough estimation of ρ_{res}^0 for Cr+1.3 at.% Si from the measurements of Galkin [1, 6, 8] on Cr + 1.3 at.% Si doped with Mn. Mn doping moves the Fermi level upwards through the impurity level (E_{imp}^+ of references [1, 4]) situated in the SDW energy gap. This results in a sharp peak in the residual resistivity at about 0.6 at.% Mn, where the Fermi level is resonant with the impurity level. The effects of the peak disappear at about 0.8 at.% Mn. On increasing the Mn content further, the Fermi energy increases more and moves farther away from the resonance condition, thereby resulting in the contribution of ρ_{res}^0 in equation (3) becoming smaller and smaller. This follows from equation (16) of reference [3] for the case where $E_{\text{imp}}^+ - E_F \gg \gamma$, where γ is the width of the impurity level. The residual resistivity of $(Cr_{1-x}Mn_x)$–1.3 at.% Si was measured by Galkin for x up to 3 at.% Mn [1, 6, 8]. For more than about 0.8 at.% Mn the residual resistivity increases approximately linearly with increasing Mn content [3]. Increasing the Mn content does not change the nature of the SDW state in $(Cr_{1-x}Mn_x)$–1.3 at.% Si. The alloys remain in the CSDW state for all x. From the above it seems reasonable to assume that a back-extrapolation of the linear part of the residual resistivity of $(Cr_{1-x}Mn_x)$–1.3 at.% Si from above $x = 0.8$ at.% Mn down to $x = 0$ will give a rough estimate of the residual resistivity $\rho_0^0/(1-\alpha)$ of Cr + 1.3 at.% Si in the absence of resonant scattering effects. A back-extrapolation of the residual resistivity from $x > 0.8$ at.% of $(Cr_{1-x}Mn_x)$–1.3 at.% Si in figure 2 of reference [6] down to $x = 0$ gives $\rho_0^0/(1-\alpha) \approx 16.6\ \mu\Omega$ cm. From figure 2 of reference [1] we obtain $\rho_{\exp}(0) \approx 19.5\ \mu\Omega$ cm for Cr + 1.3 at.% Si. Using equation (1) at 0 K and $\rho_0^0 = 15.2\ \mu\Omega$ cm (see above), one then obtains for Cr + 1.3 at.% Si the values $\rho_{\text{res}}^0 \approx 2.9\ \mu\Omega$ cm and $\alpha \approx 0.1$. This value of α obtained for the ISDW phase of Cr + 1.3 at.% Si seems to be rather low when compared to $\alpha \approx 0.3$ for other ISDW Cr alloys [9].

If resonant impurity scattering effects are absent and $\Delta\rho/\rho$ is only determined by effects of the SDW energy gap, neglecting other possible magnetic effects, then $\Delta\rho/\rho = \alpha\,\Delta(T)/\Delta(0)$. Using $\alpha = 0.1$ as an example, $\Delta\rho/\rho = \alpha\,\Delta(T)/\Delta(0)$ is plotted as a solid curve in figure 4(b) for the case of Cr + 1.2 at.% Si. The difference $(\Delta\rho/\rho)_{\exp} - (\Delta\rho/\rho)_{\alpha=0.1}$ in figure 4 gives an estimate of the combined effects of $\rho_{\text{res}}(T)$, $\rho_m(T)$ and other magnetic effects that are responsible for the first-order transition in $(\Delta\rho/\rho)_{\exp}$ for Cr + 1.2 at.% Si. In figure 4 there is a long 'tail' of relatively large $(\Delta\rho/\rho)_{\exp}$ values at $T > T_N$. The large 'tail' originates from the effects of spin fluctuations and probably also from effects of possible local impurity states that are thought to exist also at $T > T_N$ [7].

It is interesting to note the minimum in $\Delta\rho/\rho$ of Cr + 1.2 at.% Si in figure 4(b) at T_{IC} as well as the large discontinuity of about 0.09 in $(\Delta\rho/\rho)_{\exp}$ at the first-order Néel transition. Effects other than that of the SDW energy gap seem to be very large in this

crystal. In the case of Cr + 1.6 at.% Si we used the same $\alpha = 0.1$ to plot the effects of just the SDW energy gap as an example in figure 4(c). For this crystal the 'tail' above T_N in $(\Delta\rho/\rho)_{\text{exp}}$ is also very large and long. There is a discontinuity of about 0.09 in $(\Delta\rho/\rho)_{\text{exp}}$ at T_N. Also of interest for both the Cr + 1.2 at.% Si and Cr + 1.6 at.% Si crystals are the peaks in $\Delta\rho/\rho$ roughly at 100 K.

In the case of Cr + 0.5 at.% Si, we assume to a first approximation that resonant impurity scattering effects are small due to the low impurity concentration. Justification for this assumption is found in reference [1] and the present figure 3. Galkin [1] proposed that the dip in figure 3, starting at about 1 at.% Si, is due to the onset of resonant impurity scattering effects. The concentration of 0.5 at.% Si is well below this onset concentration. It was furthermore also shown by Galkin *et al* [2] that the onset of resonant impurity scattering effects is at around the triple-point concentration, $c_t \approx 1$ at.% Si, where there is a change in the concentration dependence of T_N for the Cr–Si alloy system (figure 4 of reference [2]). Assuming therefore that $\Delta\rho/\rho$ for Cr + 0.5 at.% Si at 0 K is fully determined by the value of α, we obtain from the back-extrapolation in figure 1(a) $\alpha = 0.32$, which agrees very well with α obtained previously [9] for other ISDW Cr alloys. The $\Delta\rho/\rho$–T curve calculated for SDW energy gap effects alone, using $\alpha = 0.32$, is shown by the solid curve in figure 4(a) for Cr + 0.5 at.% Si. There is again a large and long 'tail' for $(\Delta\rho/\rho)_{\text{exp}}$ above T_N due to spin-fluctuation effects as well as a peak just above 100 K, similarly to the cases for Cr + 1.2 at.% Si and Cr + 1.6 at.% Si. The origins of these peaks are currently unknown.

4.2. Cr–Ga alloys

Unfortunately there are not experiments available, like that for Cr–Si, in which ρ was measured on doping Cr–Ga alloys with V or Mn in order to study the role of resonant impurity scattering effects. We are therefore not able at present to obtain values of ρ_0^0 and ρ_{res}^0 for a proper analysis of the data for the Cr–Ga alloy crystals. In order to get some qualitative information from the resistivity data on the Cr–Ga crystals, we neglect the effects of ρ_{res}^0 in the residual resistivity of the two crystals containing 0.16 and 0.42 at.% Ga. This is in a sense justified by the relatively low impurity content of these two crystals (ρ_{res}^0 is proportional to the impurity concentration [7]) and the fact that the concentrations of both are well below the triple-point concentration (assuming that the change in the concentration dependence of T_N at c_t of Cr–Ga also signifies the onset of impurity resonance scattering effects, as for Cr–Si). For these two crystals we therefore obtained the nonmagnetic resistivity by back-extrapolation of the high-temperature measurements using equation (2) and $\rho_{\text{exp}}(0) = \rho_0^0/(1-\alpha)$ with $\alpha = 0.3$, the typical value for ISDW Cr alloys, and neglecting ρ_{res}^0. Figures 2(a) and 2(b) show the temperature dependence of the ideal nonmagnetic component of the resistivity of Cr + 0.16 at.% Ga and Cr + 0.42 at.% Ga obtained from the back-extrapolation. Figures 5(a) and 5(b) show $\Delta\rho/\rho$–T calculated from the curves of figures 2(a) and 2(b). Also shown in figures 5(a) and 5(b) are the behaviours expected if $\Delta\rho/\rho$ was determined by considering only nesting effects of the Fermi surface sheets using $\alpha = 0.3$. As in the case of Cr–Si, the two Cr–Ga crystals containing 0.16 and 0.42 at.% Ga also have large and long 'tails' in $\Delta\rho/\rho$–T at $T > T_N$. These are due to strong spin-fluctuation effects at $T > T_N$. Also of interest is the small anomaly at T_{sf} in the $\Delta\rho/\rho$–T curve of Cr + 0.16 at.% Ga as well as peaks in the vicinity of 100 K for both, similarly to the observation for the Cr–Si crystals.

For the Cr + 0.88 at.% Ga crystal ($c > c_t$), ρ_{res}^0 may not be negligibly small and we have not attempted to obtain a $\Delta\rho/\rho$–T curve for this crystal. The back-extrapolated ρ–T curve (broken curve) in figure 2(c) for this crystal was calculated using $\alpha = 0.3$ and

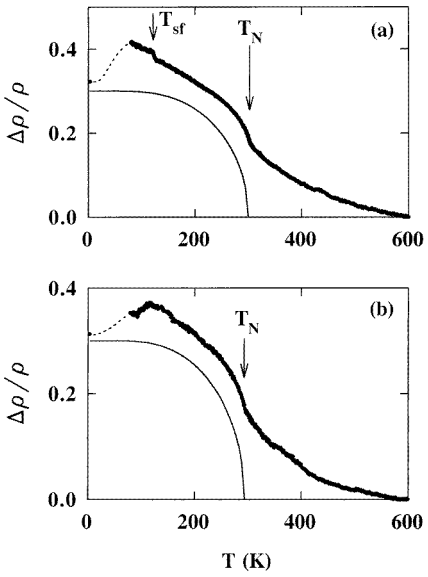

Figure 5. The resistivity anomaly, $\Delta\rho/\rho = [\rho_{\rm exp}(T) - \rho_{\rm nonmagn}(T)]/\rho_{\rm exp}(T)$, as a function of the temperature for (a) Cr+0.16 at.% Ga and (b) Cr+0.42 at.% Ga. The broken line connecting the measurements at 4.2 K to that at 77 K is a guide to the eye. The solid line in each panel was calculated with $\alpha = 0.3$ and represents the expected $\Delta\rho/\rho$ taking just nesting effects of the Fermi surface sheets into account.

$\rho^0_{\rm res} = 0$ and is only meant as a guide to the eye. It however also shows magnetic effects in Cr + 0.88 at.% Ga to persist to temperatures as high as about $2T_N$.

5. Conclusions

The present electrical resistivity (ρ) measurements on dilute Cr–Si and Cr–Ga alloy single crystals to temperatures well above the Néel point (T_N) allow for a determination of the nonmagnetic component of the electrical resistivity of these alloys. The ratio of the magnetic anomaly to the resistivity, $\Delta\rho/\rho$, was obtained for the alloys as a function of temperature. Relatively large magnetic components, up to about 15% at T_N, of the resistivity were found to persist in the alloys up to temperatures as high as $2T_N$. An interesting point is the maximum around very roughly 100 K, observed in the $\Delta\rho/\rho$–T curves of the Cr–Si and Cr–Ga alloys. Similar peaks were previously [10] also observed for Cr–Ir alloys. The origin of this behaviour is currently unknown. Also of interest is the minimum observed in $\Delta\rho/\rho$–T at the ISDW–CSDW phase transition temperature of the Cr + 1.2 at.% Si crystal and the small, nearly step-like, anomaly at the spin-flip transition temperature of the Cr + 0.16 at.% Ga crystal. Analyses of the resistivity data clearly show a relatively large component of magnetic origin, other than that due to annihilation of the nesting surfaces of the electron and hole Fermi surface sheets, to be present in the electrical resistivity of dilute Cr–Si and Cr–Ga alloys for temperatures $0 < T < 2T_N$. Spin-fluctuation effects and temperature-dependent resonant impurity scattering of electrons probably contribute to this magnetic component.

Acknowledgment

Financial aid from the South African Foundation for Research Developement is acknowledged.

References

[1] Galkin V Yu 1991 *Sov. Phys.–Solid State* **33** 1622
[2] Galkin V Yu, Tugushev V V and Tugusheva T E 1991 *Sov. Phys.–Solid State* **33** 4
[3] Fawcett E and Galkin V Yu 1991 *J. Phys.: Condens. Matter* **3** 7167
[4] Galkin V 1989 *J. Magn. Magn. Mater.* **79** 327
[5] Galkin V Yu and Fawcett E 1993 *J. Magn. Magn. Mater.* **119** 321
[6] Galkin V Yu 1993 *Int. J. Mod. Phys.* B **7** 638
[7] Fawcett E, Alberts H L, Galkin V Yu, Noakes D R and Yakhmi J V 1994 *Rev. Mod. Phys.* **66** 25
[8] Galkin V Yu 1987 *Phys. Met. Metallogr.* **64** 150
[9] Chiu C H, Jericho M H and March R H 1971 *Can. J. Phys.* **49** 3010
[10] Martynova J, Alberts H L and Smit P 1996 *J. Phys.: Condens. Matter* **8** 10 473
[11] Arajs S and Katzenmeyer W E 1967 *J. Phys. Soc. Japan* **23** 932
[12] Fukamichi K 1979 *J. Phys. F: Met. Phys.* **9** L85
[13] Kaneko T, Shirakawa K and Fukamichi K 1982 *J. Appl. Phys.* **53** 2459
[14] Prinsloo A R E, Alberts H L and Smit P 1997 *J. Phys.: Condens. Matter* **9** 9961
[15] Prinsloo A R E, Alberts H L and Smit P 1997 *Phys. Rev.* B **56** 11 777
[16] Anderson R A, Alberts H L and Smit P 1993 *J. Phys.: Condens. Matter* **5** 1733
[17] Nye J F 1957 *Physical Properties of Crystals* (Oxford: Clarendon) pp 4, 22
[18] Cabrera G G 1977 *J. Phys. F: Met. Phys.* **7** 827
[19] Nascimento L C S and Cabrera G G 1981 *J. Low Temp. Phys.* **45** 481
[20] Rossiter P L 1987 *The Electrical Resistivity of Metals and Alloys* (Cambridge: Cambridge University Press)
[21] Mott N F and Jones H 1958 *The Theory of the Properties of Metals and Alloys* (New York: Dover) p 274
[22] Mühlschlegel B 1959 *Z. Phys.* **155** 313